Relative Navigation with Laser-Based Intermittent Measurement for Formation Flying Satellites

Jongwoo Lee, Dae-Eun Kang, Sang-Young Park

Abstract—This study presents a precise relative navigational method for satellites flying in formation using laser-based intermittent measurement data. The measurement data for the relative navigation between two satellites consist of a relative distance measured by a laser instrument and relative attitude angles measured by attitude determination. The relative navigation solutions are estimated by both the Extended Kalman filter (EKF) and unscented Kalman filter (UKF). The solutions estimated by the EKF may become inaccurate or even diverge as measurement outage time gets longer because the EKF utilizes a linearization approach. However, this study shows that the UKF with the appropriate scaling parameters provides a stable and accurate relative navigation solutions despite the long measurement outage time and large initial error as compared to the relative navigation solutions of the EKF. Various navigation results have been analyzed by adjusting the scaling parameters of the UKF.

Keywords—Satellite relative navigation, laser-based measurement, intermittent measurement, unscented kalman filter.

I. INTRODUCTION

SATELLITES in formation benefit from advantages such as a long baseline, a flexible configuration, and a reasonable cost of production and launch, and have made significant contributions [1], [2]. In satellite formation flying missions, precise relative navigation that provides a relative position and velocity of each satellite is essential. A laser instrument has recently been receiving attention because of its ability to measure a relative distance between satellites in formation with a high level of precision [3]–[5]. This precisely measured relative distance may help to improve the performance of relative navigation. In a numerical simulation, it has been shown that laser-based relative navigation with consecutive measurement using the extended Kalman filter (EKF) for a pair of satellites provided precise relative navigational solutions [6].

For consecutive measurement, however, a satellite equipped with a laser instrument must have precise aim. Otherwise, especially in the cases where the satellites are far from each other, measurement failure is possible. Reference [7] shows that in the case where consecutive laser-based measurement data cannot be obtained, a long measurement outage time negatively affects the performance (i.e. the accuracy and stability) of relative navigation using the EKF. Dynamic and measurement models undergo linearization in the EKF

Jongwoo Lee and Dae-Eun Kang are with the Astrodynamics & Control Laboratory, Department of Astronomy, Yonsei University, Seoul 03722, Republic of Korea (e-mail: jongwoo@yonsei.ac.kr, rkdeodms@gmail.com).

Sang-Young Park is with Astrodynamics & Control Laboratory, Department of Astronomy, Yonsei University, Seoul 03722, Republic of Korea (corresponding author, phone: +82-2-2123-5687; fax: +82-2-392-7680; e-mail: spark624@yonsei.ac.kr).

formulation. If a time step of measurement is short, the EKF simplifies and approximates a nonlinear system well [8]. Otherwise, the errors derived from the linearization accumulate.

Motivated by the problem posed by EKF degradation, we have studied laser-based relative navigation for satellites in formation using the unscented Kalman filter (UKF). Based on the unscented transformation (UT), the UKF approximates the state distribution using sigma points, and propagates the sigma points through a true nonlinear system. In this fashion, the UKF addresses the inherent flaws of the EKF caused by its linearization approach [9], [10].

Relative navigation using a laser instrument with the EKF and the relative navigation using gyro-sensors and a vision sensor with the UKF have been proposed [6], [11]. The performance of laser-based relative navigation with intermittent measurement using the batch filter has also previously been studied [7]. The objective of this study is to analyze the performance of the UKF with intermittent measurement for the laser-based relative navigation of satellites in formation.

The rest of the paper is organized as follows. Section II introduces the dynamic and measurement models necessary for the relative navigation for a pair of satellites. The formulation of the UKF is given in Section III. Section IV illustrates the simulation results of the laser-based relative navigation using both the UKF and the EKF. Finally, Section V states the conclusions and gives the directions for future works.

II. RELATIVE NAVIGATION

A. Dynamic Model

In order to build a precise relative navigation algorithm with a precise dynamic model, the two-body equation including the perturbations has been introduced, as described in (1) [6].

$$\ddot{\vec{r}} = -\frac{\mu_E}{|\vec{r}|^3}\vec{r} + \vec{a}_{geo} + \vec{a}_{drag} + \vec{a}_{3rd} + \vec{a}_{SRP} \qquad (1)$$

where μ_E represents the standard gravitational parameter of the Earth. $\vec{r}$ and $\ddot{\vec{r}}$ represent the absolute position vector and the absolute acceleration vector of a satellite in the Earth-centered inertial (ECI) frame, respectively. The ECI frame has been defined as J2000. $\vec{a}_{geo}$, $\vec{a}_{drag}$, $\vec{a}_{3rd}$, and $\vec{a}_{SRP}$ indicate the perturbations caused by the aspherical property of the Earth, the air resistance, the gravitation from the Sun and the Moon, and the solar radiation pressure, respectively. The JGM3 and the exponential model are employed for $\vec{a}_{geo}$ and $\vec{a}_{drag}$, respectively. For $\vec{a}_{3rd}$ and $\vec{a}_{SRP}$, we have referred to Reference

World Academy of Science, Engineering and Technology
International Journal of Aerospace and Mechanical Engineering
Vol:12, No:2, 2018

[12]. The orbit or the state vector of the satellite consisting of the position and the velocity represented in the ECI frame, can be propagated by integrating (1).

This study considers a pair of satellites in formation, the chief satellite and the deputy satellite. Because the relative distance and attitude are measured in the spherical frame, the relative state vector represented in the spherical frame is necessary. The relative state vector of the deputy with respect to the chief represented in spherical frame is defined as in (2),

$$\vec{X}_{rel,sph} = \begin{bmatrix} \rho & \theta & \phi & \dot{\rho} & \dot{\theta} & \dot{\phi} \end{bmatrix}^T \tag{2}$$

where ρ is a relative distance, and θ and ϕ are the azimuth and elevation of the deputy with respect to the chief, respectively. $\dot{\rho}, \dot{\theta}, \dot{\phi}$ are the rate of ρ, θ, ϕ, respectively. $\vec{X}_{rel,sph}$ can be calculated as follows. The relative state vector between the two satellites in the ECI frame $\vec{X}_{rel,ECI}$ is calculated by differencing the two absolute state vectors represented in the ECI frame [13]. Then, $\vec{X}_{rel,ECI}$ is transformed into the RTN frame with respect to the chief. Finally, the relative state vector represented in the RTN frame $\vec{X}_{rel,RTN}$ is transformed into the spherical coordinates as $\vec{X}_{rel,sph}$. A more detailed description of the transformations between the frames can be found in [6] and is not repeated here for conciseness.

B. Laser-Based Measurement

In this study, to simulate the relative distance of the measurement data, the software that simulates the femtosecond laser instrument has been used [6]. This instrument uses the principle of synthetic wavelength interferometry (SWI) and is expected to yield a distance measurement value with µm to cm level accuracy depending on distance [14]. The laser software used for this study may yield a distance measurement value with an error of a mean of about 10 µm and a standard deviation of about 100 µm in 1 σ up to a distance of 10 km [15]. As the distance increases above 10 km, the mean becomes unstable and the standard deviation increases linearly in log scales. A more detailed description of the femtosecond laser instrument itself can be found in [16].

The azimuth and the elevation corresponding to a laser direction were assumed to be obtained via the attitude determination of the chief. The algorithm of the attitude determination has not been discussed in this study. Instead, the uncertainty in the attitude determination has been introduced. This uncertainty, represented by Gaussian random errors with zero mean and a standard deviation of a certain value, has been added to the true azimuth and elevation [6].

III. Estimation Algorithm

A. Nonlinear Discrete-Time System

Consider a nonlinear discrete-time system consisting of the dynamic and measurement models as:

$$\dot{\vec{X}}_k = f(\vec{X}_k) + \vec{v}_k \tag{3}$$

$$\vec{y}_k = h_k(\vec{X}_k) + \vec{\omega}_k \tag{4}$$

where $k \in \mathbb{N}$ indicates a time step, $\vec{X}_k \in \mathbb{R}^n$ indicates a state vector, and $\vec{y}_k \in \mathbb{R}^m$ indicates a measurement vector. The nonlinear functions f and h_k are the dynamic and measurement models of the system, respectively. The variables $\vec{\omega}_k \in \mathbb{R}^n$ and $\vec{v}_k \in \mathbb{R}^m$ denote a process noise with a covariance matrix Q and a measurement noise with a covariance matrix R, respectively.

In this study, the dynamic model used to propagate the relative state represented in the spherical frame $\vec{X}_{rel,sph}$ follows the process in Section II.A. The absolute states of the chief and the deputy consisting of the position and the velocity represented in the ECI frame, $\vec{X}_{A,ECI}$ and $\vec{X}_{B,ECI}$, are propagated by integrating the equation of motion in (1). A nonlinear discrete-time system with the equation of motion in (1) is described as in (5):

$$\dot{\vec{X}}_{A/B,ECI,k} = f(\vec{X}_{A/B,ECI,k}) + \vec{v}_{ECI,k} \tag{5}$$

where f is the two-body equation including the perturbations described as in (1). By differencing the two propagated states $\vec{X}_{A,ECI,k+1}$ and $\vec{X}_{B,ECI,k+1}$, the propagated relative state represented in the ECI frame can be calculated.

$$\vec{X}_{rel,ECI,k+1} = \vec{X}_{A,ECI,k+1} - \vec{X}_{B,ECI,k+1}. \tag{6}$$

By transforming the ECI frame into the RTN frame, and then the spherical frame, the propagated relative state represented in the spherical frame $\vec{X}_{rel,sph}$ can be obtained [6].

This study assumes that $\vec{X}_{A,ECI}$ is obtained by the GPS navigation system at every moment, and $\vec{X}_{B,ECI}$ is obtained through a transformation with $\vec{X}_{A,ECI}$ and $\vec{X}_{rel,sph}$ [6], [14].

The measurement model h_k is described in (7).

$$h_k = H = \begin{bmatrix} 1 & 0 & 0 & sf & 0 & 0 \\ 0 & 1 & 0 & 0 & 0 & 0 \\ 0 & 0 & 1 & 0 & 0 & 0 \end{bmatrix}. \tag{7}$$

As seen in (7), the measurement model h_k is the time-invariant linear model H. Since the relative distance and attitude are measured directly, if the inter-satellite alignment to receive the laser signal is made exactly, the measurement model H is $[I_{3x3} \ 0_{3x3}]$. Adding the scale factor sf to H gets rid of the drift due to the relative distance rate [6].

The process noise and the measurement noise are additive and uncorrelated to each other.

B. Unscented Kalman Filter with Intermittent Measurement

Both the EKF and the UKF approximate a state distribution using a Gaussian random variable (GRV) [16]. In the EKF, the mean of a GRV is propagated through a first-order linearized nonlinear system. If the time step of a measurement is short, the EKF simplifies and approximates a nonlinear system well [8]. Otherwise, this first-order linearization may induce large errors

World Academy of Science, Engineering and Technology
International Journal of Aerospace and Mechanical Engineering
Vol:12, No:2, 2018

in the mean and the corresponding error covariance of the propagated GRV. In addition, as the initial error or the nonlinearity of the system increases, the EKF may provide suboptimal performance or even diverge [8], [16]. On the contrary, the UKF represents the Gaussian state distribution using sigma points, based on the UT. The UKF propagates the sigma points through a true nonlinear system, so that the UKF is able to propagate the mean and the corresponding error covariance of the GRV accurately to the 3rd order in the Taylor series expansion for all nonlinearities [16].

The distribution of the sigma points is determined by the scaling parameters α, β, κ, and λ. α determines the spread of the sigma points around the mean of the GRV. κ is a secondary scaling parameter. β is used to incorporate the prior knowledge of the distribution of the GRV. λ is determined by $\lambda = \alpha^2(n + \kappa) - n$ where n is the dimension of the state vector [16]. The filtering performance of the UKF, such as accuracy and convergence in state estimation, significantly relies on the scaling parameters [17]. Therefore, setting the scaling parameters is a major issue when applying the UKF. α is usually set to a small positive value as $0 \leq \alpha \leq 1$. A variety of the results depending on α are presented in the next session. $\beta = 2$ is optimal for Gaussian distributions. κ is typically set to 0 or $3 - n$ 16. We have set $\kappa = 3 - n$ to minimize the difference between the moments of the standard Gaussian and the sigma points up to the fourth order [18]. The detailed algorithm and equations of the UKF may be found in [16].

In this study, we address laser-based relative navigation for satellites flying in formation by using the UKF with intermittent measurement. In general, relative navigation algorithms assume consistent measurement [14], [16], [19]. As such, the estimation algorithms based on the Kalman filter implement both the prediction and the measurement update steps at an instant k. It is possible, however, for measurement to fail due to a failure of the inter-satellite alignment, especially in cases where the satellites are distant from each other. In the case that there is no measurement data, it is not possible to implement the measurement update step. Therefore, in this study, if the laser-based measurement data are available at a certain instant k, both the prediction step and the measurement update step in the UKF are implemented. Otherwise, only the prediction step is implemented [7].

IV. NUMERICAL SIMULATIONS AND ANALYSIS

A. Relative Navigation Simulations

In order to analyze the performance of the UKF with intermittent measurement on the relative navigation for the satellites flying in formation, a pair of satellites, the chief and the deputy have been utilized. The chief orbits the Earth at an altitude of about 600 km, and the deputy is in a chief-centered projected circular orbit (PCO) with a radius of 10 km. It has been assumed that only the chief is equipped with the femtosecond laser instrument.

The true state of the satellite was set by numerical integration of the dynamic model as defined in (1). For the true state, (1) considers the aspherical property of the Earth of degree and

order of 20×20. In addition to $\vec{a}_{geo}$, $\vec{a}_{drag}$, $\vec{a}_{3rd}$, and $\vec{a}_{SRP}$, the perturbation driven by the unknown acceleration $\vec{a}_{unknown}$ with a magnitude of 10^{-14} m/s^2 has been added to (1) since the true state may never truly be known [6]. The dynamic model for the relative navigation algorithms is the two-body equation including only the J_2 gravitational perturbation in order to reduce the computational burden when considering the real-time navigation.

Since the scaling parameters have a great influence on the filtering performance of the UKF, the simulations were run while adjusting the scaling parameters. Because the influence of α is dominant over β, κ, and λ [17], we have adjusted only α, and set $\beta = 2$ and $\kappa = 3 - n$. λ is determined by $3\alpha^2 - 6$.

Because this study addresses the filtering performance with intermittent measurement, the simulations with different measurement outage times have been implemented. The laser-based measurement outage time was assumed not to change over the course of the simulation. For example, if the outage time is 10 seconds, the laser-based measurement data are obtained at every interval of 10 seconds during the simulation. The simulation time was set to 6000 seconds.

B. Results

In the simulation case 1, the uncertainty of the attitude determination has been assumed to be 1". Because this uncertainty suggests uncertainty in laser direction, it yields a limitation on relative navigation. The initial relative state has been found by adding the initial state estimation error to the true state. The initial errors correspond to about 20 m and 20 cm/s for the relative position and the relative velocity between the satellites, respectively. The initial error covariance matrix P_0 has been defined as in (8),

$$P_0 = M_{error}^2 \qquad (8)$$

where M_{error}^2 is a diagonal matrix in which its diagonal entries are equal to the initial state estimation error. Q and R have been empirically determined to improve the performance. For identification, these conditions are termed Case 1. Fig. 1 shows the various estimation errors in the relative position while adjusting α for Case 1. The estimation errors in the relative position in the present paper are presented by the root mean square (RMS) of the 3D relative position estimation errors represented in the RTN frame at the instants when the measurement data are obtained throughout the simulation time. The numbers in the legend in Fig. 1 denote the measurement outage period. As shown in Fig. 1, the errors in $\alpha < 1 \times 10^{-3}$ are worse than in the larger α. The UKF with the appropriate scaling parameter $(3 \times 10^{-5} \leq \alpha \leq 1 \times 10^{-4})$ maintains the accuracy of the relative navigation solution, regardless of the measurement outage time. The proposed algorithm with $\alpha \leq 2 \times 10^{-5}$ was unable to be implemented since the error covariance matrix at a certain instant k was not a positive semi-definite, i.e. the matrix was not a true error covariance matrix.

A similar result may be seen in a different condition. In Case 2, the uncertainty of the attitude determination has been

World Academy of Science, Engineering and Technology
International Journal of Aerospace and Mechanical Engineering
Vol:12, No:2, 2018

assumed to be 0.001°. The initial errors in this case correspond to about 1 km and 20 cm/s for the relative position and the relative velocity between the satellites, respectively. The initial error covariance matrix has been the same as in Case 1. Q and R have been empirically determined to improve the performance. Fig. 2 shows the various estimation errors in the relative position while adjusting α for Case 2. The numbers in the legend in Fig. 2 denote the measurement outage period. In Case 2, the UKF with the appropriate scaling parameter ($3 \times 10^{-5} \leq \alpha \leq 7 \times 10^{-5}$) maintains the accuracy of the relative navigation solution regardless of the measurement outage period, as shown in Fig. 2. However, the smaller the value of α, the more accurate the result is.
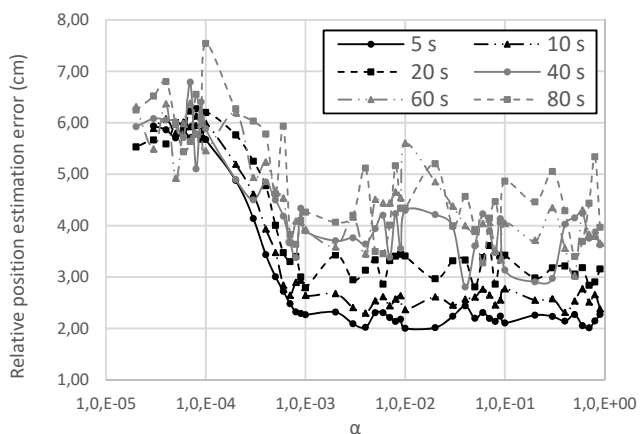

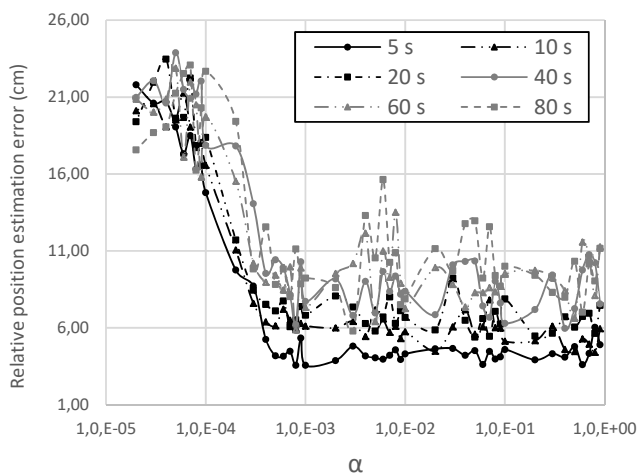Fig. 1 Various estimation errors in the relative position while adjusting α for Case 1

Fig. 2 Various estimation errors in the relative position while adjusting α for Case 2

The sigma points which are too close to the mean of the GRV consider the nonlinearity only near the mean. The propagation of these sigma points is similar to the mean-propagating of the EKF and leads the UKF to sub-optimal estimation. Therefore, the accuracies of the estimation results in $\alpha > 10^{-3}$ is better than those in $\alpha < 10^{-3}$.

To prove the performance of the proposed algorithm, we performed the simulations for Case 1 and Case 2 again and compared the results from the UKF with those from the EKF. The optimal α within the UKF was set by 1×10^{-2}. As shown in Fig. 3, the error performances of the UKF are much less sensitive to laser-based measurement outage time than those of the EKF. The superiority of the estimation performance by the UKF over the EKF is more noticeable when the initial error becomes large. At a measurement outage time of 80 s, the UKF reduces the estimation error of the EKF by 70.34% for the simulation case 1 and 94.74% for the case 2.
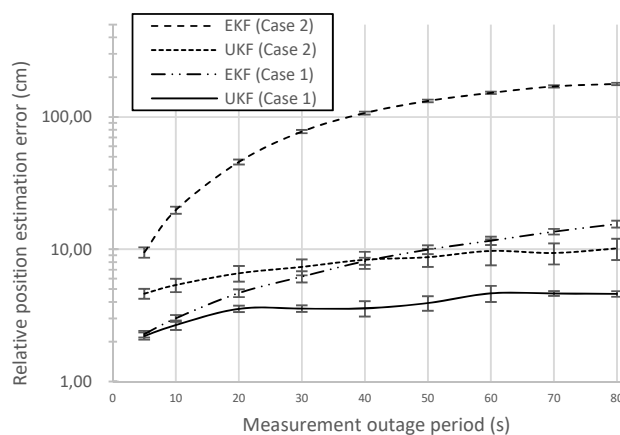

Fig. 3 Various estimation errors in relative position by the UKF and the EKF for Case 1 and Case2

V. CONCLUSION

In the present paper, using the UKF with intermittent measurement for the precise laser-based relative navigation of the satellites in formation was studied and applied to a pair of satellites in a PCO with a radius of 10 km. The relative distance was measured by the femtosecond laser instrument carried by the chief satellite, and the relative attitude angles were measured by attitude determination of the chief satellite. The numerical simulations demonstrated that the UKF with appropriate scaling parameters continues to provide a stable and accurate relative navigation solution despite a long measurement outage time and large initial error when compared to the relative navigation solution of the EKF. This study shows that the UKF may overcome the inherent problem of the degradation of the EKF as measurement outage time increases. In future studies, estimation performances under different conditions should be analyzed.

REFERENCES

[1] B. D. Tapley, S. Bettadpur, J. C. Ries, P. F. Thompson, and M. M. Watkins, "GRACE measurements of mass variability in the Earth system," *Science*, vol. 305, no. 5683, pp. 503–505, July 2004.
[2] G. Krieger, A. Moreira, H. Fiedler, I. Hajnsek, M. Werner, M. Younis, and M. Zink, "TanDEM-X: A satellite formation for high-resolution SAR interferometry," *IEEE Trans. Geoscience and Remote Sensing*, vol. 45, no. 11, pp. 3317–3341, Oct. 2007.
[3] D. A. Shaddock, "Space-based gravitational wave detection with LISA," *Classical and Quantum Gravity*, vol. 25, no. 11, pp. 114012-1–114012-11, May 2008.

World Academy of Science, Engineering and Technology
International Journal of Aerospace and Mechanical Engineering
Vol:12, No:2, 2018

[4] B. S. Sheard, G. Heinzel, K. Danzmann, D. A. Shaddock, W. M. Klipstein, and W. M. Folkner, "Intersatellite laser ranging instrument for the GRACE follow-on mission," *Journal of Geodesy*, pp. 1–13, May 2012.

[5] X. Wang, D. Gong, L. Xu, X. Shao, and D. Duan, "Laser radar based relative navigation using improved adaptive Huber filter," *Acta Astronautica*, vol. 68, no. 11, pp. 1872–1880, June–July 2011.

[6] S. Jung, S.-Y. Park, H.-E. Park, C.-D. Park, S.-W. Kim, and Y.-S. Jang, "Real-time determination of relative position between satellites using laser ranging," *Journal of Astronomy and Space Sciences*, vol. 29, no. 4, pp. 351–362, Dec. 2012.

[7] J. Lee, D.-E. Kang, S.-Y. Park, Y. Lee, and P. Kim, "Laser-based spacecraft relative navigation with intermittent observation data," in *Proc. KSSS 2017 Spring Conference*, Byunsan, Republic of Korea, 2017, pp. 78–83.

[8] D.-J. Lee and K. T. Alfriend, "Precise real-time orbit estimation using the unscented Kalman filter," in *Proc. AAS/AIAA Space Flight Mechanics Meeting*, Ponce, Puerto Rico, 2003, pp. 1853–1872.

[9] S. J. Julier and J. K. Uhlmann, "A new extension of the Kalman filter to nonlinear systems," in *Proc. AeroSense: 11th International Symposium on Aerospace/Defense, Sensing, Simulation and Controls*, Orlando, FL, United States, 1997, pp. 182–193.

[10] R. Van Der Merwe and E. A. Wan, "The square-root unscented Kalman filter for state and parameter-estimation," in *Proc. International Conference on Acoustics, Speech, and Signal Processing*, Salt Lake City, UT, United States, 2001, pp. 3461–3464.

[11] L. Zhang, T. Li, H. Yang, S. Zhang, H. Cai, and S. Qian, "Unscented Kalman filtering for relative spacecraft attitude and position estimation," *The Journal of Navigation*, vol. 68, no. 3, pp. 528–548, May 2015.

[12] D. A. Vallado and W. D. McClain, *Fundamentals of Astrodynamics and Applications*, Hawthorne, California: Microcosm Press, 2013, pp. 574–584.

[13] S. Leung and O. Montenbruck, "Real-time navigation of formation-flying spacecraft using global-positioning-system measurements," *Journal of Guidance Control and Dynamics*, vol. 28, no. 2, pp. 226–235, Mar. 2005.

[14] K. Lee, H. Oh, H.-E. Park, S.-Y. Park, and C. Park, "Laser-based relative navigation using GPS measurements for spacecraft formation flying," *Journal of Astronomy and Space Sciences*, vol. 32, no. 4, pp. 387–393, Dec. 2015.

[15] Kang, D.-E., Park, S.-Y., and Lee, J., "A satellite relative navigation based on hardware characteristics of femtosecond laser," in *Proc. the 3rd World Congress on Mechanical, Chemical, and Material Engineering (MCM'17)*, Rome, Italy, pp. ICMIE 119-1– ICMIE 119-6, June 2017.

[16] Y.-S. Jang, K. Lee, S. Han, J. Lee, Y.-J. Kim, and S.-W. Kim, "Absolute distance measurement with extension of nonambiguity range using the frequency comb of a femtosecond laser," *Optical Engineering*, vol. 53, no. 12, pp. 122403-1–122403-6, May 2014.

[17] E. A. Wan and R. Van Der Merwe, "The unscented Kalman filter for nonlinear estimation," in *Proc. IEEE Symposium 2000 (AS-SPCC)*, Lake Louise, AB, pp. 153–158, Oct. 2000.

[18] S. Julier, J. Uhlmann, and H. F. Durrant-Whyte, "A new method for the nonlinear transformation of means and covariances in filters and estimators," *IEEE Trans. automatic control*, vol. 45, no. 3, pp. 477–482, Mar. 2000.

[19] H. Oh, H.-E. Park, K. Lee, S.-Y. Park, and C. Park, "Improved GPS-based satellite relative navigation using femtosecond laser relative distance measurements," *Journal of Astronomy and Space Sciences*, vol. 33, no. 1, pp. 45–54, Mar. 2016.